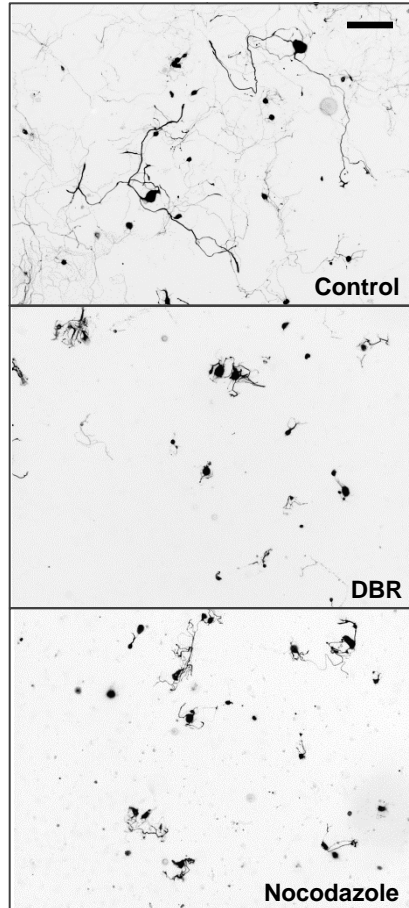
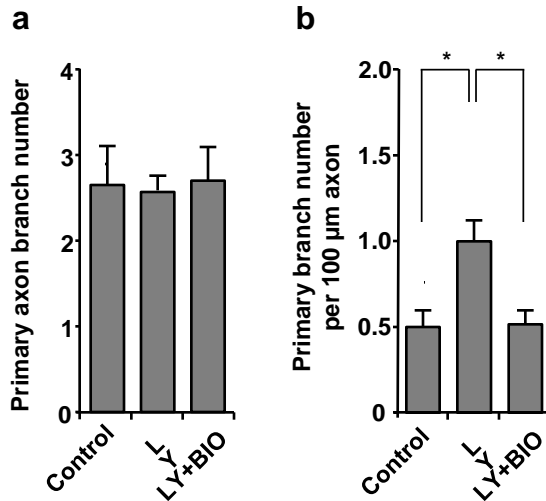


**Images after initial 3-day-culture
(before replating)**



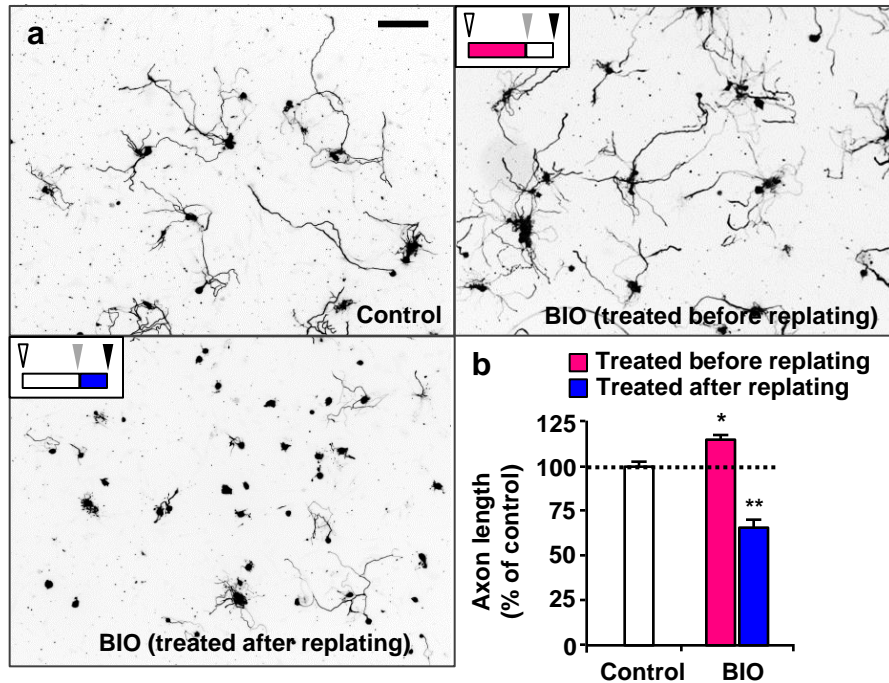
Supplementary Figure S1. Axon growth requires both gene transcription and microtubule dynamics.

Representative images of adult DRG neurons after the initial 3-day-culture period of the culture-and-replating protocol (see **Fig. 1a**). Neurons were cultured in the presence or absence of dichlorobenzimidazole riboside (DBR, 20 μ M), nocodazole (50 nM), or a vehicle control (DMSO), as indicated. Note that treatment of neurons with either DBR or nocodazole drastically prevents axon growth. Scale bar, 200 μ m.



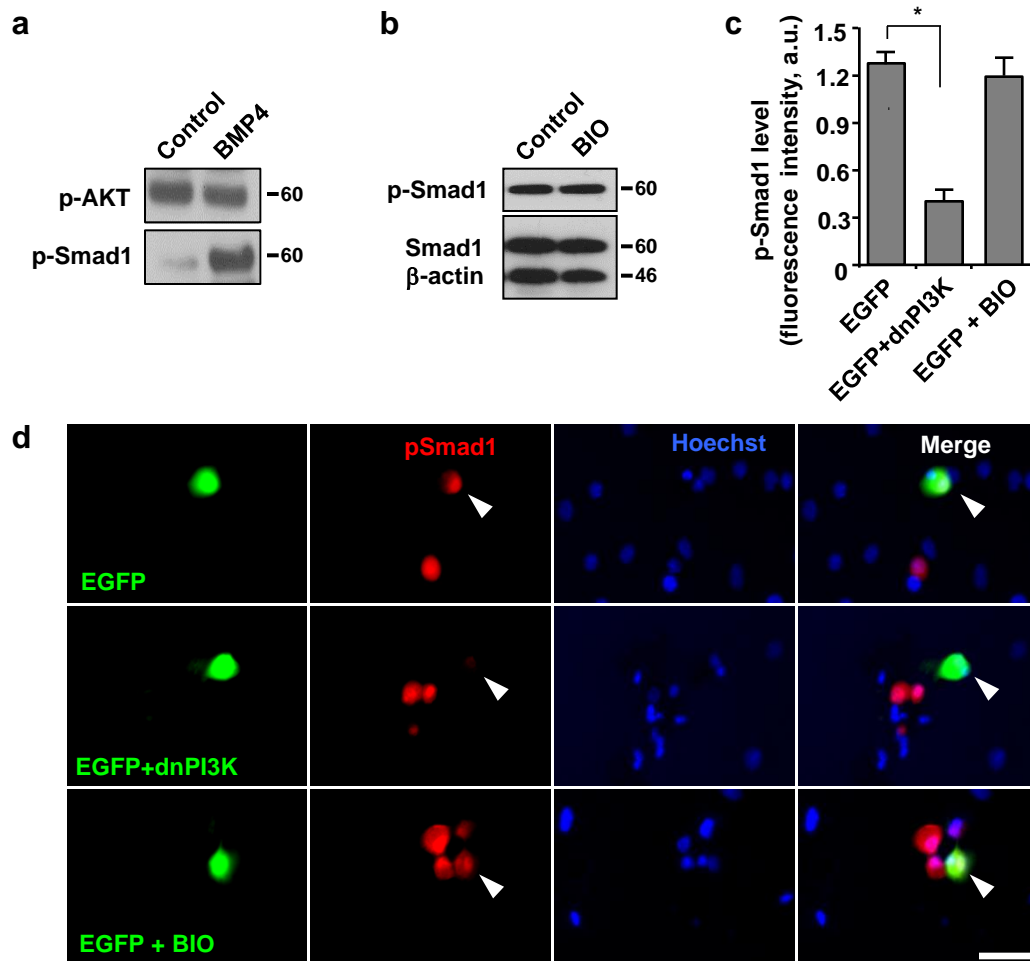
Supplementary Figure S2. Effects of LY294002 and 6-bromoindirubin-3'-acetoxime (BIO) on axonal branch formation.

(a, b) Adult DRG neurons were dissociated, cultured for 3 days, and then replated to induce axon growth anew, as depicted in **Fig. 1a**. Neurons were grown in the presence or absence of LY294002 (LY, 10 μ M) and/or 6-bromoindirubin-3'-acetoxime (BIO, 500 nM), as indicated, during the initial 3-day-culture period. Drugs were washed out at the time of replating and neurons were cultured in the absence of drugs thereafter. Neurons were fixed at 20 hr after replating and the number of axonal branches was quantified. Data represent mean \pm s.e.m. from three independent experiments ($n = 3$ for each experimental condition). * $p < 0.05$, unpaired two-tailed Student's t-test.



Supplementary Figure S3. Effects of suppression of GSK3 activity on regenerative axon growth.

(a, b) Adult DRG neurons were dissociated, cultured for 3 days and then replated to initiate axon growth anew, as depicted in Fig. 1a. Neurons were treated with 6-bromindirubin-3'-acetoxime (BIO, 500 nM) or vehicle control (DMSO) either before (red bar in b) or after replating (blue bar in b), as indicated, and axon length was measured at 20 hr after replating. The schematics and symbols (upper left insets in a) are identical to Fig. 1d. Representative images of replated neurons are shown in a, and quantification of axon length after replating is shown in b. Scale bar, 200 μ m. Data represent mean \pm s.e.m. from three independent experiments (n = 3 for each experimental condition). * p < 0.05 compared to control, ** p < 0.01 compared to control, unpaired two-tailed Student's t-test.

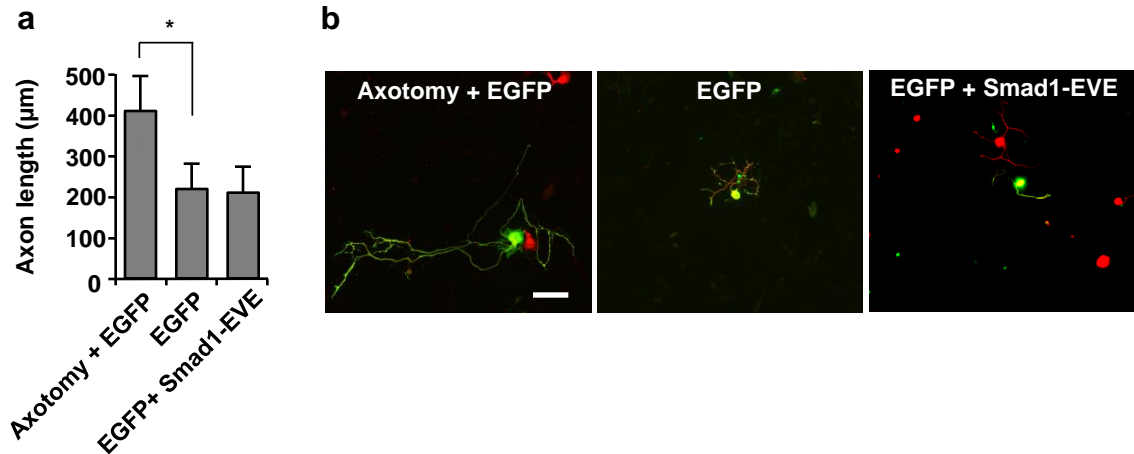


Supplementary Figure S4. BMP4 and PI3K-GSK3 signalling employ distinct mechanisms to activate Smad1.

(a) Dissociated adult DRG neurons were treated with BMP4 (100 ng/ml, 4 hr) or vehicle control, as indicated, and then subjected to Western blot to monitor the levels of phospho-AKT (p-AKT) and phospho-Smad1 (p-Smad1). Representative immunoblots are shown.

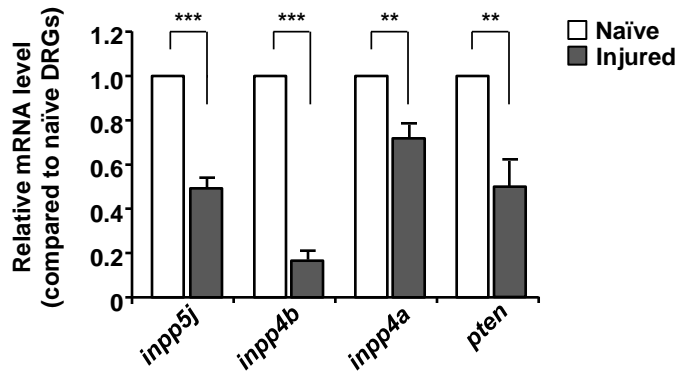
(b) Dissociated adult DRG neurons were treated with 6-bromoindirubin-3'-acetoxime (BIO) (500 nM, 3 days) or vehicle control, as indicated, and then subjected to Western blot analysis to monitor the levels of phospho- and total-Smad1. Actin antibodies were used as a loading control. Representative immunoblots are shown.

(c, d) Adult DRG neurons were transfected with either EGFP alone or together with dnPI3K, and replated 3 days after transfection. Neurons were cultured overnight in the presence or absence of BIO (500 nM), as indicated. Immunocytochemical analysis was performed to examine nuclear accumulation of phospho-Smad1. Quantification (c) and representative images (d) of phospho-Smad1 in the nucleus are shown. Transfected cells are marked by arrowheads. Scale bar, 50 μ m. Data represent mean \pm s.e.m. from three independent experiments (n = 3 for each experimental condition). * p < 0.05, unpaired two-tailed Student's t-test.



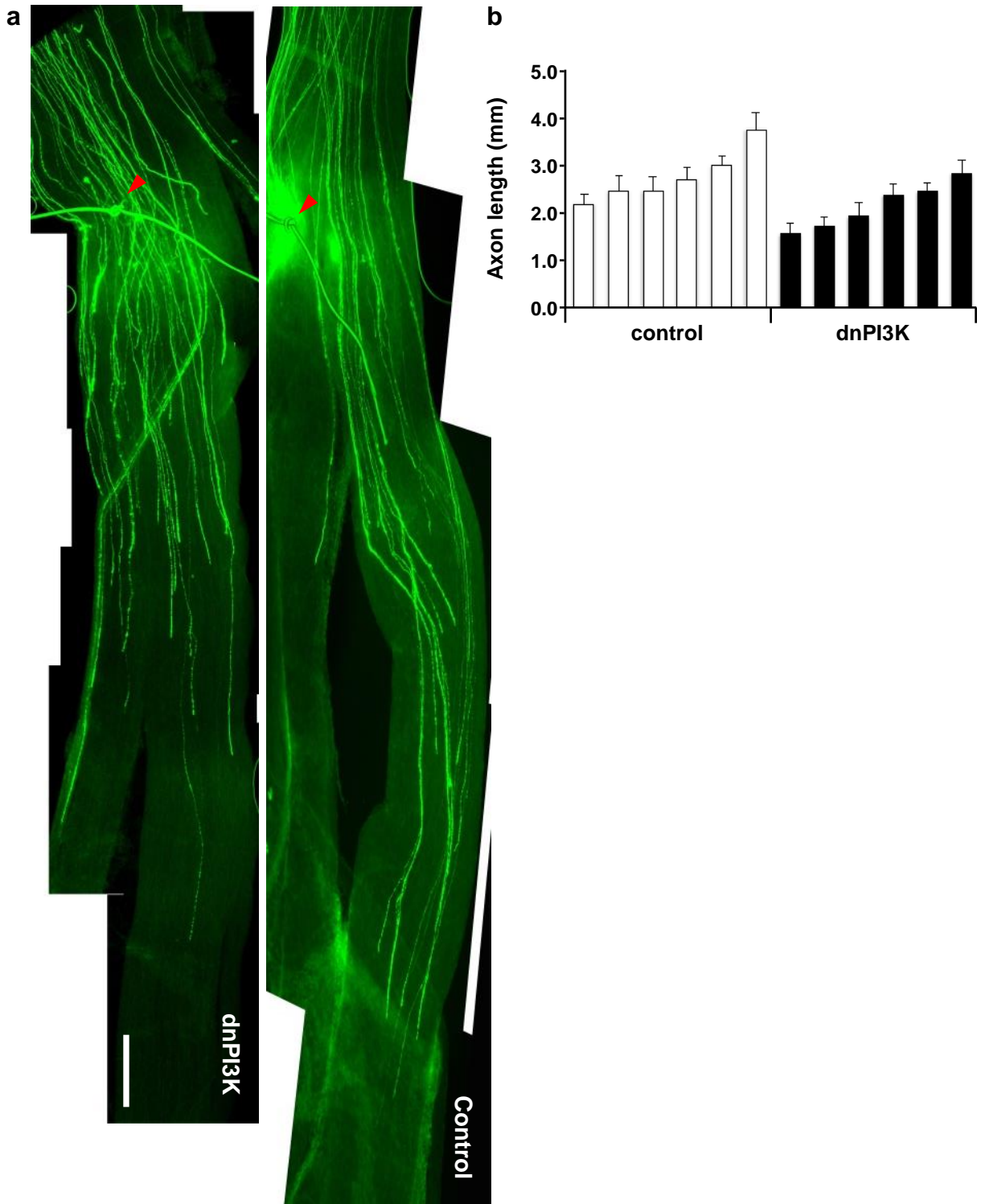
Supplementary Figure S5. Effect of a phospho-mimetic form of Smad1 on axon growth potential.

(a, b) L4 and L5 DRGs of adult mice were electroporated *in vivo* with either EGFP alone or together with a phospho-mimetic form of Smad1 (Smad1-EVE). At 3 days after *in vivo* electroporation, L4 and L5 DRGs were dissected out, dissociated, and cultured overnight. Neurons were fixed at 20 hr after culture and immunostained for neuronal tubulin β III, TuJ1 (red). Transfected neurons are shown in green. Quantification of axon length (a) and representative images (b) are presented. Scale bar, 200 μ m. Data represent mean \pm s.e.m. from three independent experiments ($n = 3$ for each experimental condition). * $p < 0.01$, unpaired two-tailed Student's t-test.

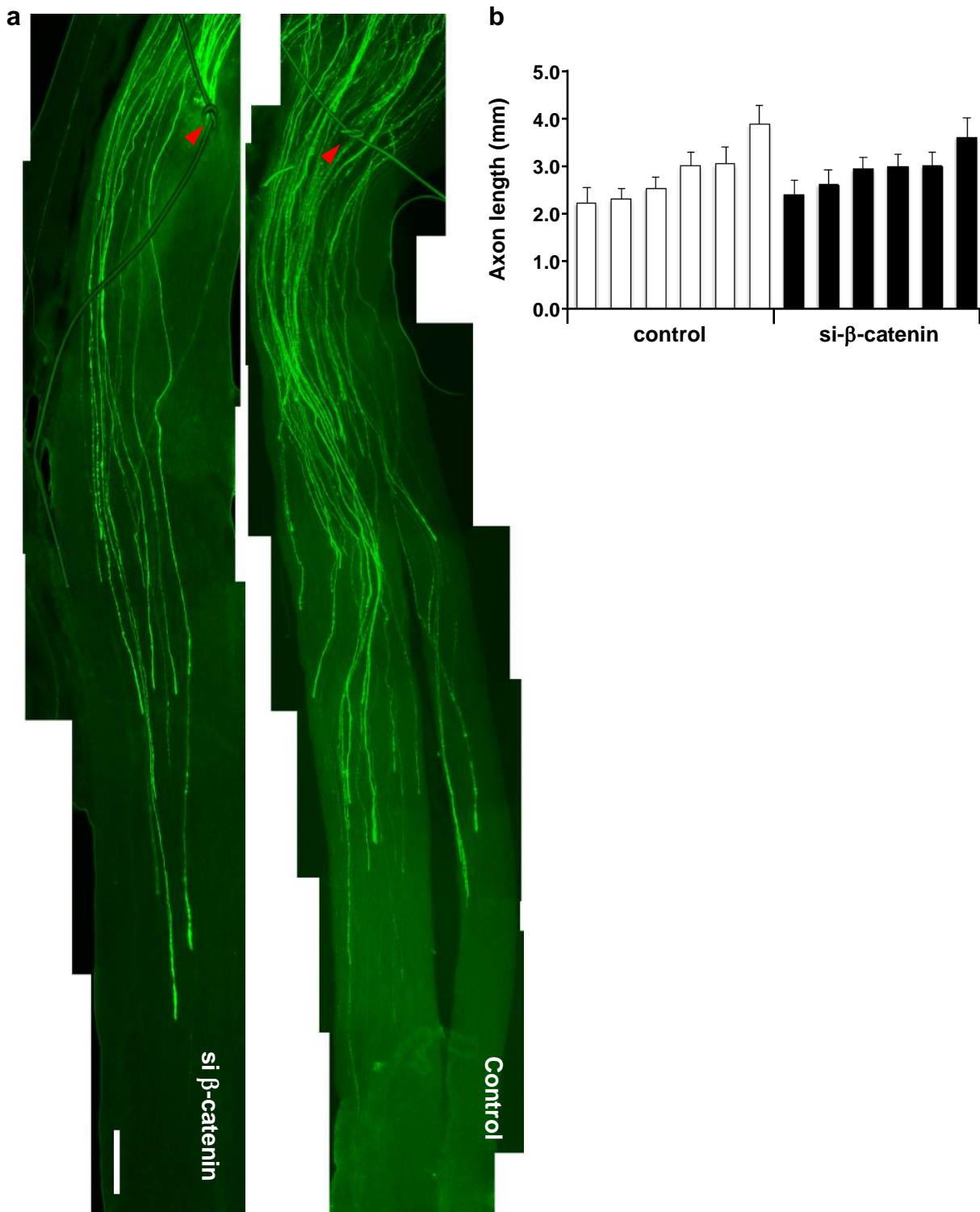


Supplementary Figure S6. Peripheral axotomy down-regulates mRNA levels of inositol phosphatases.

L4 and L5 DRGs from naïve and conditioning lesioned mice were subjected to quantitative real time polymerase chain reaction to examine the mRNA levels of *pten*, *inpp4a*, *inpp4b* or *inpp5j*, as indicated. Data represent mean \pm s.e.m. from three independent experiments (n = 3 for each experimental condition). ** p < 0.01; *** p < 0.001, unpaired two-tailed Student's t-test.



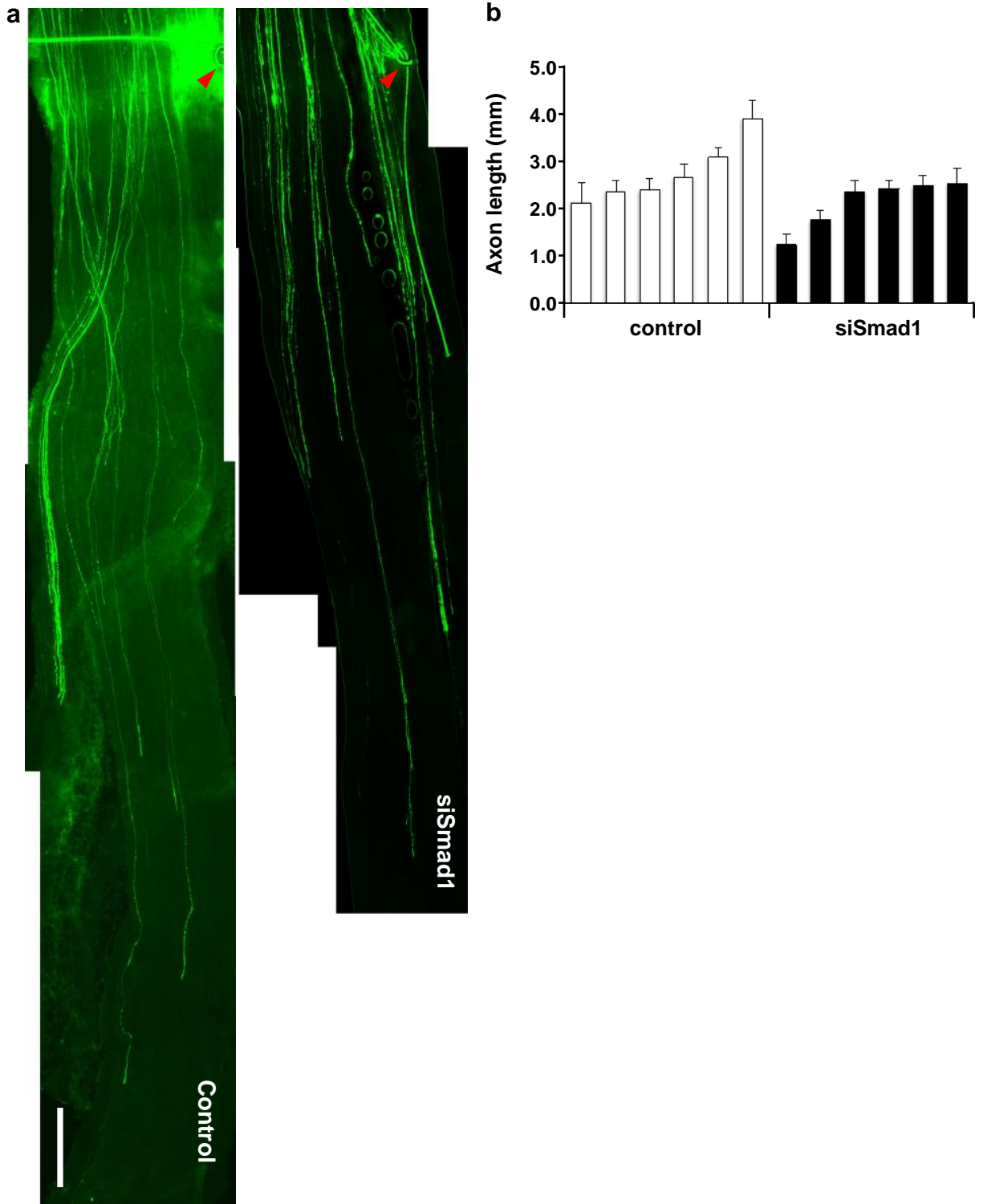
Supplementary Figure S7. Effect of disruption of PI3K signalling on axon regeneration *in vivo*.
(a) Enlarged high resolution images of whole-mount nerve segments presented in Fig. 3c. Scale bar, 500 μm .
(b) Individual mouse data for Fig. 3b. Each bar depicts mean \pm s.e.m. value of the length of axon regeneration measured from individual mouse transfected *in vivo* with either EGFP alone (control) or together with dnPI3K. n = 6 mice for each experimental condition.



Supplementary Figure S8. Effect of β -catenin depletion on axon regeneration *in vivo*.

(a) Enlarged high resolution images of whole-mount nerve segments presented in Fig. 6e. Scale bar, 500 μ m.

(b) Individual mouse data for Fig. 6d. Each bar depicts mean \pm s.e.m. value of the length of axon regeneration measured from individual mouse transfected *in vivo* with either EGFP alone (control) or together with siRNAs against β -catenin. n = 6 mice for each experimental condition.



Supplementary Figure S9. Effect of Smad1 depletion on axon regeneration *in vivo*.

(a) Enlarged high resolution images of whole-mount nerve segments presented in Fig. 8c. Scale bar, 500 μ m.

(b) Individual mouse data for Fig. 8b. Each bar depicts mean \pm s.e.m. value of the length of axon regeneration measured from individual mouse transfected *in vivo* with either EGFP alone (control) or together with siRNAs against Smad1. n = 6 mice for each experimental condition.

Fig. 1b

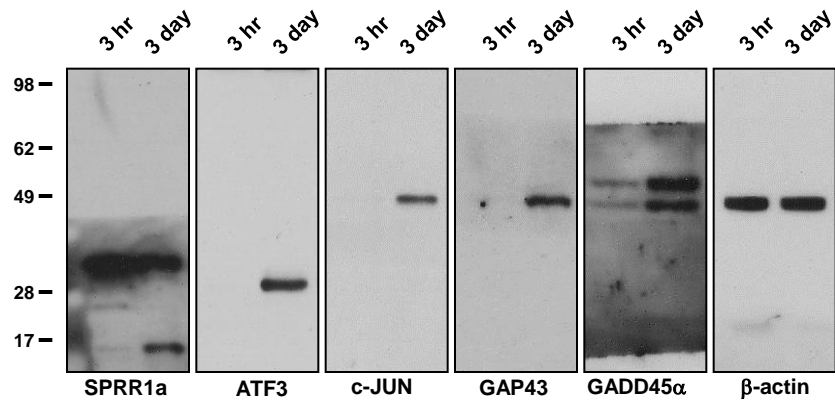


Fig. 2d

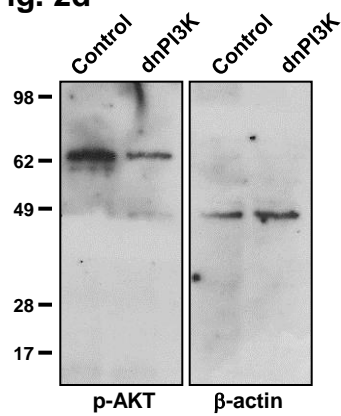


Fig. 2g

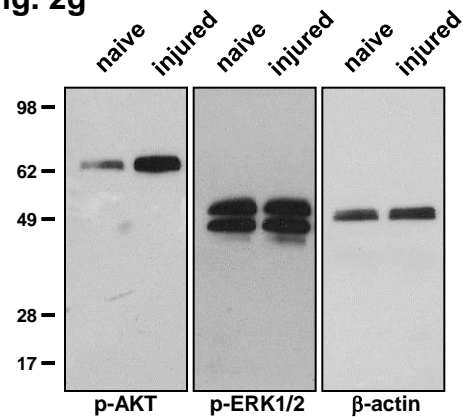
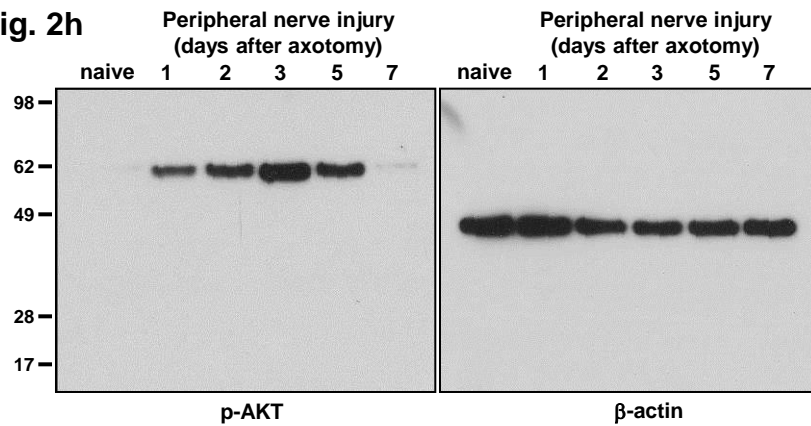


Fig. 2h



Supplementary Figure S10. Full scan images of western blot data in Fig. 1-2.

Fig. 4d

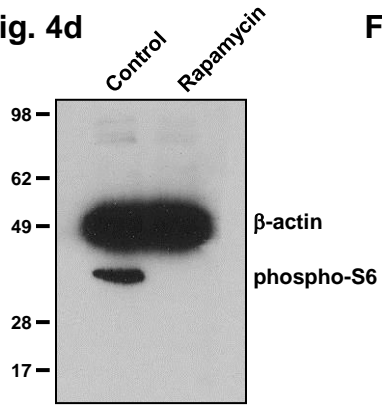


Fig. 5a

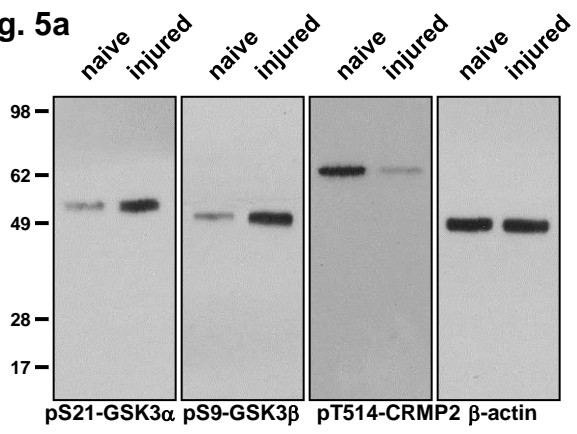


Fig. 5b 3-day-culture

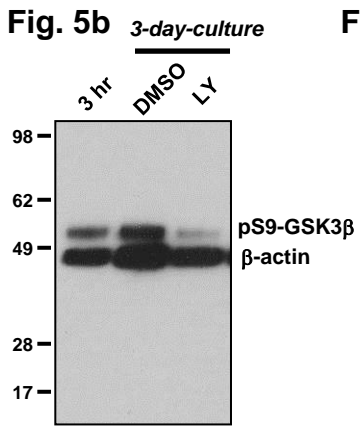


Fig. 6a

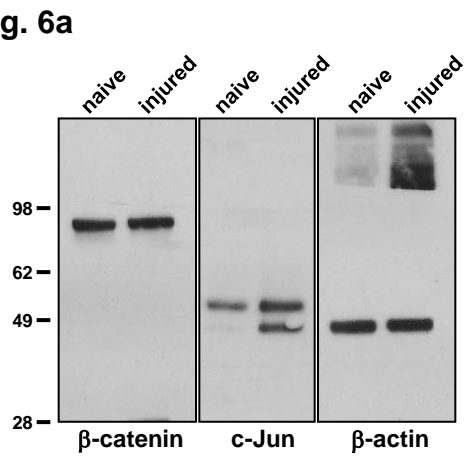


Fig. 6b 3-day-culture

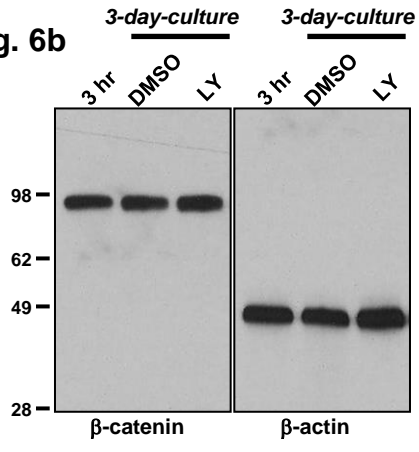
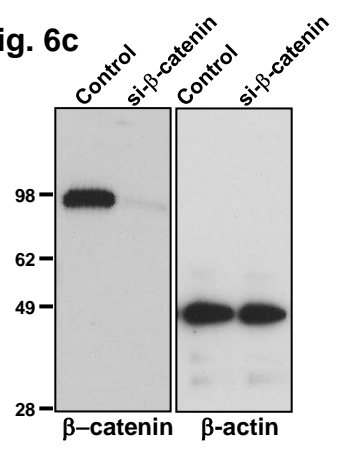


Fig. 6c



Supplementary Figure S11. Full scan images of western blot data in Fig. 4-6.

Fig. 7a

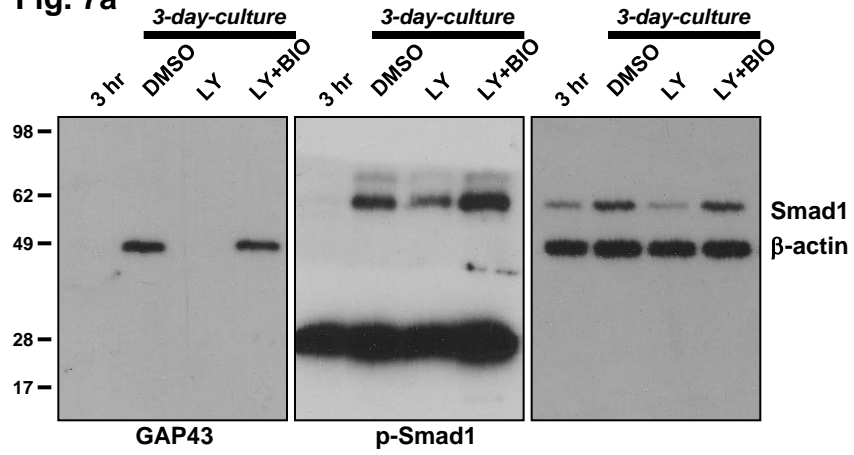


Fig. 7e

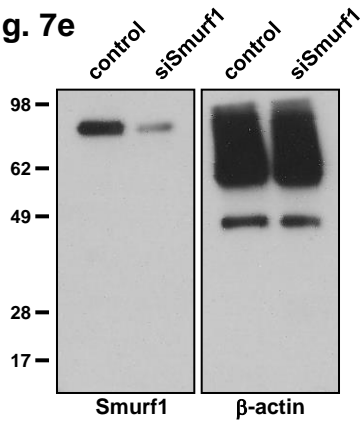


Fig. 8a

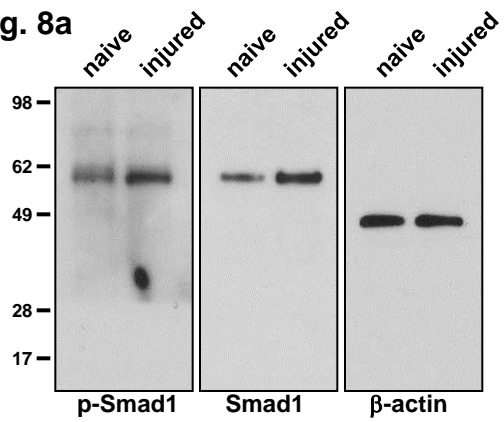
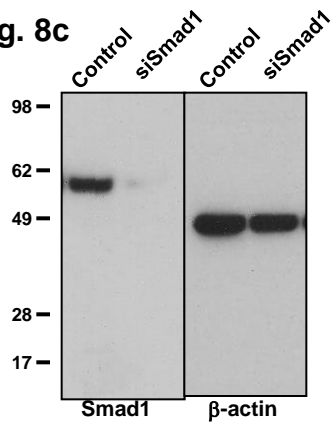


Fig. 8c



Supplementary Figure S12. Full scan images of western blot data in Fig. 7-8.